Inner-scaled turbulent statistics of turbulent pipe flows

Junsun Ahn, Jae Hwa Lee and Hyung Jin Sung*

Department of Mechanical Engineering, KAIST
291 Daehak-ro, Yuseong-gu, Daejeon 305-701, Korea
junsun_ahn@kaist.ac.kr, jhlee06@kaist.ac.kr, hjsung@kaist.ac.kr

ABSTRACT

Direct numerical simulations (DNSs) of fully developed turbulent pipe flows for Re_τ=180, 544, and 934 were performed to investigate the inner-scaled turbulent statistics associated with spatial amplitude modulation (AM). A long streamwise domain length, 30*R*, was adopted to avoid the domain length effect, which affects on the convergence of turbulence statistics. The present result shows that the near-wall peak in the streamwise turbulence intensity increases with increasing the Reynolds number. This trend is very consistent to turbulent boundary layer (TBL) and channel flows, indicating that there is a universal flow behavior in turbulent canonical flows. Evidence to support this finding is found in pre-multiplied energy spectra and two-point AM covariance. It is determined that both the long wavelength energy near the wall and the non-linear effects of AM contribute to the growth of the near-wall peak in the streamwise turbulence intensity.

INTRODUCTION

Many studies have agreed that the near-wall peak value in the streamwise turbulence intensity of a TBL significantly increases with the Reynolds number (for example, Marusic & Kunkel, 2003). The found of Schlatter & Örlü (2010b) also supported for this conclusion in their study of the DNS of TBLs. Hoyas & Jiménez (2006) provided evidence in support of this trend in the peak intensity for turbulent channel flows by DNS. However, there is no clear trend of the streamwise intensity peak in turbulent pipe flows. Ng et al. (2011) conducted hot-wire experiments on turbulent channel and pipe flows and found the increase in the streamwise turbulence intensity. On the contrary, in turbulent pipe flows, Hultmark et al. (2010) and Hultmark et al. (2012) reported that the magnitude of the streamwise peak value seems to be nearly constant. This difference might come from the experimental uncertainties. It has been proposed the limitations on the ability of experiments to produce reliable statistics for near-wall turbulent flows and to resolve their turbulence structures. Ligrani & Bradshaw (1987) suggested a hot-wire length of $l^+ \leq$ 20-25 and a value of $l/d \geq 200$, where $l^+=lu_\tau/\nu$ and d is the diameter of the hot-wire probe. Hutchins et al. (2009) also suggested that the overall temporal resolution (t^+) of the measurement system should be less than $t^+\approx 3$. For instance, the parameters of several experiments in turbulent pipe flow seem to fall outside these limits of l/d and t^+, and they might likely result in ambiguous values.

The near-wall peak in the streamwise turbulence intensity has been focused on previous many studies since it is a useful parameter for the characterization of the interactions between the inner and outer regions, and so is also a key point of the present study. It has been known that there is an interaction between the near-wall and outer flows, which can be represented in terms of the non-linear AM signature, i.e., the degree to which the small-scale signal is modulated by the large-scale signal. Mathis et al. (2009a) proposed a one-point AM coefficient based on the Hilbert transform and found that in TBLs this coefficient increases with the Reynolds number. Mathis et al. (2009b) also compared the AM coefficients of TBLs and those of channel and pipe flows, and concluded that the flow interaction mechanism is invariant even though the scales of these flow structures differ. However, Hultmark et al. (2010) and Hultmark et al. (2012) argued that the constant inner peak in the streamwise turbulence intensity for turbulent pipe flows indicates that the flow mechanism in turbulent pipe flows is different from those of TBLs. They suggested that the energy balances in the two types of flows are fundamentally different, i.e., that turbulence production is shifted away from the wall in turbulent pipe flows. The continuing conflict over these issues triggered our efforts to improve the DNS of turbulent pipe flows.

In the present study, we concentrate on the behavior of the inner-scaled near-wall peak in the turbulence intensity, especially the streamwise turbulence intensity, in turbulent pipe flows. We performed DNSs of fully developed turbulent pipe flows up to 30*R* in length for Re_τ=180, 544, and 934. The streamwise mean velocity profiles and the turbulence intensities are plotted with respect to the Reynolds number to elucidate statistical behavior. The pre-multiplied energy spectra and the two-point AM covariance of the streamwise velocity fluctuations support the claim that the near-wall peak in the streamwise turbulence intensity increases with the Reynolds number. This finding implies that the flow interactions between the modulating large-scale and modulated small-scale structures in pipe flows are similar to those in TBL and channel flows.

NUMERICAL METHOD

The incompressible and fully developed turbulent pipe flow was modeled with the Navier-Stokes equations and the continuity equation in cylindrical coordinates. The governing equations were non-dimensionalized by the maximum velocity of the fully developed laminar profile (U_c) and the pipe radius (R). The Reynolds numbers based on the pipe diameter (D) and the bulk velocity (U_b) are Re_D=5300, 19000, and 53000 (180, 544 and 934 based on Re_τ). The governing equations were integrated in time by using the fractional step method with the implicit velocity decoupling procedure proposed by Kim et al. (2002) and

Jang et al. (2011). No-slip conditions were used for the velocities at the wall and periodic boundary conditions were applied in the streamwise and azimuthal directions to the fully developed turbulent pipe flow. The centerline condition for the radial velocity was obtained by averaging the corresponding values across the centerline (Akselvoll & Moin, 1996). z, r, and θ are the flow axial direction, the radial coordinate measured along the pipe axis, and the azimuthal coordinate; u_z, u_r, and u_θ are the corresponding velocity components. For convenience, we defined the axial coordinate x=z, the wall-normal coordinate y=1-R, and the spanwise coordinate z=$r\theta$. This spanwise arc length has previously been discussed by Wu et al. (2012). In addition, it was helpful to introduce the analogous velocity components u=u_z, v=–u_r, and w=u_θ.

For Re_τ=180 and 934, the wall-normal grid distributions were the same as those used by Wu & Moin (2008). For Re_τ=544, the minimum and maximum spacings in the wall units were determined to be 0.176 and 4.284 at r=R and 0.415R respectively. The velocity fields were initialized with a laminar mean velocity profile, and random fluctuations were superimposed on the maximum amplitude of 30% of the maximum velocity. For Re_τ=180 and 544, the time steps ($\Delta tU_c/R$) were changed from 0.0002 to 0.03 and 0.02 respectively after the first 3,000 time steps. For Re_τ=934, the time step was 0.0004 during the first 400 time steps. These parameters were chosen to accommodate the start-up effects associated with the imposed unrealistic initial velocity fields. After the first calculation, the computational time steps for Re_τ=180, 544, and 934 were fixed at Δt =0.03, 0.02, and 0.01 respectively, and the maximum axial CFL component was set at 1.25. The simulations for Re_τ=180, 544, and 934 were run initially for 13,000R/U_c, 10,000R/U_c and 32,000R/U_c respectively to eliminate flow transient processes, and the individual averaged statistics were sampled during the last 114,000Δt, 105,000Δt, and 174,000Δt respectively by using 64 parallel processors (IBM p595) at the KISTI supercomputer center. Each sampling time duration was sufficient to allow a particle to travel more than 25 times along the full axial domain of the pipes at a velocity equal to the bulk velocity.

The axial lengths of the computational domains were adjusted to 30R as long as Wu et al. (2012) since previous experimental studies have shown that the maximum wavelength of very-large-scale motions is 8-16R for pipe flows (Kim & Adrian, 1999; Guala et al., 2006). Chin et al. (2010) also examined the effects of the pipe axial domain length on turbulence statistics and suggested that for Re_τ=170 and 500 at least 8πR is sufficient for convergence turbulence statistics, even in the correlation in the inner and outer regions. This long domain reduced the effects of domain length on the turbulence statistics.

MEAN FLOW STATISTICS

In this section, we obtained the mean flow statistics to investigate the trends of the inner-scaled turbulent mean statistics. The mean velocity and log-law indicator function profiles are shown in figure 1, including those of Wu et al. (2012) and Wu & Moin (2008) for Re_τ=685 and 1142 respectively All the mean velocity profiles are in good agreement along the near-wall and logarithmic regions,

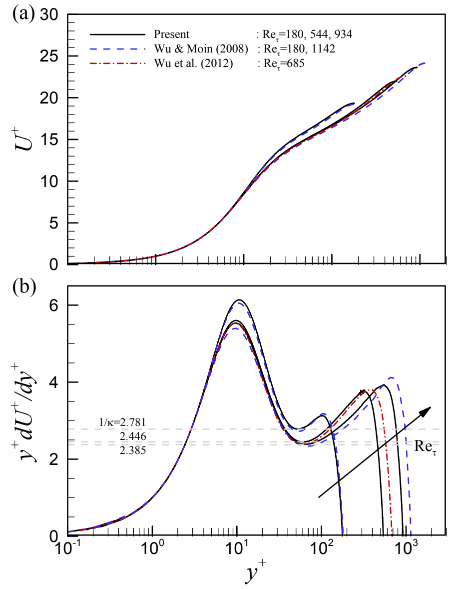

Figure 1: Mean axial velocity profiles and log-law indicator functions in the inner coordinates.

except at the lowest Reynolds number. In case of Re_τ=180, the logarithmic region is largely absent, in contrast to the results for the higher Reynolds numbers. This result is consistent with the turbulence statistics of channel flows due to the low-Reynolds-number effects (Moser et al., 1999). The log-law indicator function y^+dU^+/dy^+ is an alternative form of the mean velocity, and is a good standard for the validation of the quality of DNS results because it is more sensitive than untreated mean velocity profiles with respect to the wall-normal direction. The profiles well collapse from the wall to $y^+\approx 70$, and the local maximum value at the upper bound of the logarithmic region increases with the Reynolds number. It is well-known that a local minimum value in the logarithmic region is the same as the inverse of the von Kármán coefficient ($1/\kappa$). However, unfortunately, the present results cannot provide to determine an exact value of $1/\kappa$ because the Reynolds numbers here are not enough high. It should be noted that the universality of κ is still debated; so more DNS research at higher Reynolds numbers is needed.

Figure 2 shows the turbulence intensities and Reynolds shear stress profiles in the inner coordinates. The magnitude of the profiles increases with increase in the Reynolds number. All profiles for the range Re_τ=544 to 1142 are in good agreement in the viscous sublayer (y^+<10). The profiles of the lowest Reynolds number, Re_τ=180, show significant difference from the other profiles, which is the same pattern as the mean velocity. However, the wall-normal and spanwise intensities for Re_τ=544 slightly deviate from those of higher Reynolds numbers due to the moderate-Reynolds-number effect, as is the case for the channel flows described by Hoyas & Jiménez (2006). Figure 3 displays the variations of the peak value in the turbulence intensities and Reynolds stress with respect to the Reynolds number. All parameters increase with increase in the Reynolds number although the increasing rates differently vary. From the lowest to highest Reynolds numbers, it is shown that the growth of the streamwise

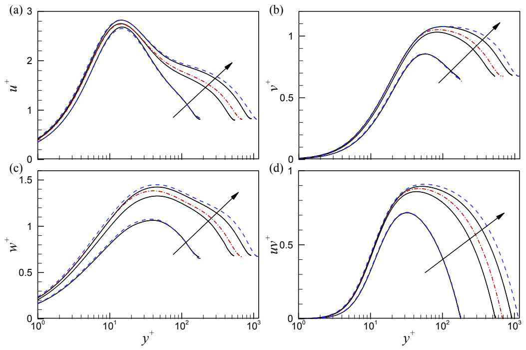

Figure 2: Turbulence intensities and Reynolds shear stress profiles in the inner coordinates. See the legend in Figure 1.

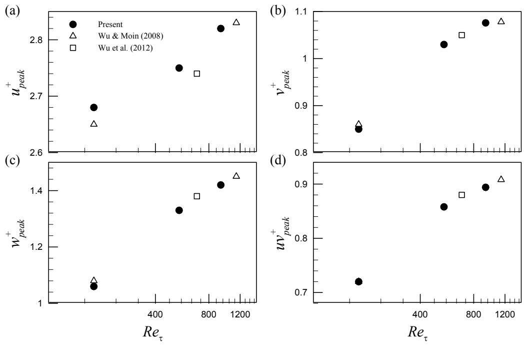

Figure 3: The peak values of the Reynolds stresses as a function of the Reynolds number.

turbulence intensities is approximately 5%, although that in the other profiles reaches up to 20%. Since the variation in the streamwise turbulence intensity is smaller than those of the others, it is difficult to be revealed from experiments due to the possibility of including measurement errors (Ligrani & Bradshaw, 1987; Hutchins et al., 2009). The trend of the streamwise turbulence intensity in the present DNS data is contrary to the previous experimental results (Hultmark et al., 2010; Hultmark et al., 2012), which suggested that the inner peak of the streamwise intensities remains approximately constant: 2.7 and 2.99 for $690<Re_\tau<3336$ and $1900<Re_\tau<99000$ respectively, whereas the outer peak increases. Based on this finding, they proposed a new flow mechanism in pipe flows that the location of turbulence production near the wall moves toward the outer region when Reynolds number increases. However, it should be remarked the near-wall peak value in their studies gradually increases within the range of the targeted Reynolds numbers. This represents that the experimental measurement might conceal the exact result. In contrast, Ng et al. (2011) reported that the near-wall peak in the streamwise turbulence intensity obviously increases from 2.65 to 2.80 with the Reynolds number in the range of $1000<Re_\tau<3100$, which is a supportive result on the present work. In addition, the DNS studies of Wu & Moin (2008) and Chin et al. (2010) have shown the similar increasing trends of the inner-scaled near-wall peak in the streamwise turbulence intensity with varying the Reynolds number.

Figure 4 exhibits the variation of the inner-scaled near-wall peak values in the streamwise turbulence intensity in pipe, channel and TBL flows from available DNS results.

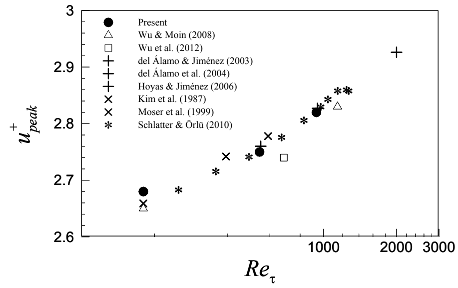

Figure 4: The peak values of the streamwise intensity as a function of the Reynolds number in pipe, channel and TBL flows.

Increasing trends of each flow are quantitatively identical regardless of flow type. In other words, the growing trend seems one function of the Reynolds number. This demonstrates that there might be a universal flow interaction in the wall-bounded turbulent flows since the near-wall peak value in the streamwise turbulence intensity is the outcome of the highest turbulence production.

SPECTRAL ANALYSIS

To provide clear evidence supporting our assertion for the increasing trend of the streamwise turbulence intensity, spectral analyses were conducted. The definition of the energy spectra was based on Wu et al. (2012). Figure 5 shows the contour plots of the pre-multiplied streamwise energy spectra of the streamwise velocity fluctuations and the one-dimensional pre-multiplied streamwise energy distributions at y^+=15 for Re_τ=180, 544, and 934. Figure 5(a) contains distinct inner peaks located at $y^+\approx15$ and the streamwise wavelength $\lambda_x^+\approx1000$, where the positions of the peaks are similar but subtly distinct due to the low-Reynolds-number effect. It has been common that the inner peak (inner site) occurs due to the near-wall cycle of streaks and quasi-streamwise vortices (Hutchins & Marusic, 2007a). Recent experimental studies have shown that the presence of the outer peak (outer site) is closely associated with very-large-scale motions (VLSMs) or superstructures in the logarithmic region (Kim & Adrian, 1999; Hutchins & Marusic, 2007b; Monty et al., 2009). The outer peak is however not present here because the Reynolds numbers employed here are not sufficiently high to fully separate the inner and outer sites. Hutchins & Marusic (2007b) proposed that complete scale-separation between the inner and outer sites can be achieved at $Re_\tau\gtrsim1700$, and being of the outer peak leads to the necessity of DNS at higher Reynolds number. The one-dimensional pre-multiplied streamwise energy spectra at y^+=15 are shown in figure 5(b). The two curves well collapse at short wavelengths, although this spectra-scaling is not suitable for the lowest Reynolds number flow. The area under the on-dimensional energy spectrum curve is equivalent to the mean-square fluctuation at the same location (here is the maximum turbulence production spot). Since the long wavelength energy increases with increasing the Reynolds number, it is confirmed that the increased near-wall peak in the streamwise intensity with the Reynolds number is attributed to the increase of the large-scale energy in the near-wall

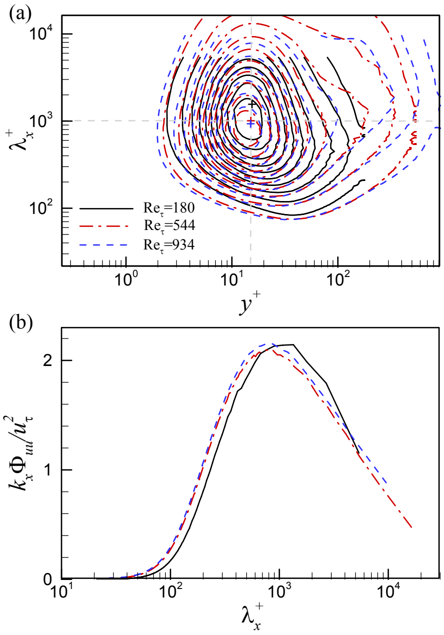

Figure 5: Pre-multiplied streamwise energy spectra of streamwise turbulence fluctuations (a) along the logarithmic abscissa and (b) at y^+=15.

region.

We also employed two-point AM covariance to identify the origin of the near-wall peak increase in the streamwise turbulence intensity. The effects of the large-scale motions in the logarithmic region on the small scales in the near-wall region can be identified with AM. AM is obtained by the scale separation and the Hilbert transform. Based on a cutoff wavelength, a raw signal is separated to the short- and long-wavelength components. The small-scale motion is again manipulated with the Hilbert transform to extract its envelope. Finally, AM is established by the correlation between the envelope of the small-scale signal (u_{EL}) and the large-scale signal (u_L) (Mathis et al., 2009a). Recently, Bernardi & Pirozzoli (2011) suggested two-point AM covariance, $C_{AM}^{2p}(y_1, y_2) = \overline{u_L(y_1)u_{EL}(y_2)}$, which can interpret the interaction between the modulated and modulating signals in the near-wall and outer regions simultaneously. The modulating influence of an off-wall location (y_1) on another location (y_2) was determined between the large-scale velocity at y_1 and the low-pass filtered envelope at y_2. Noted that since one-point AM coefficient resembles the velocity skewness, it might not be a suitable mean for unambiguously detecting or quantifying the effects of AM (Schlatter & Örlü, 2010a). Before the calculation of the two-point AM covariance, a cutoff wavelength should be needed to determine a separation criterion between the large- and small-scale motions. We firstly obtained the pre-multiplied spanwise energy spectra of the streamwise velocity fluctuations for Re_τ=180 and 934 in figure 6. Both spectra include the near-wall peak near $y^+\approx15$ and the spanwise wavelength $\lambda_z^+\approx100$, which indicates the spanwise wavelength of the streaks, the typical characteristics of near-wall cycle. The main difference between figure 6(a) and

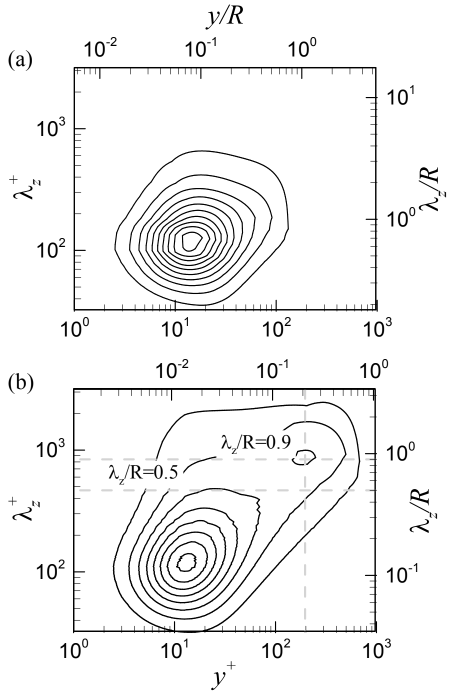

Figure 6: Contour plots of the pre-multiplied spanwise energy spectra for (a) Re_τ=180 and (b) Re_τ=934.

6(b) is the presence of the secondary peak in the logarithmic region at Re_τ=934. The outer peak is located at $y^+\approx200$ and the associated spanwise wavelength is $\lambda_z/R\approx0.9$, which is similar to the result of Wu et al. (2012). This peak verifies the organization of the very-large-scale motions in the spanwise direction (Bernardi & Pirozzoli 2011). The outer peak in the spanwise spectra also suggests that the regular near-wall large-scale motion develops faster in the spanwise direction than in the streamwise direction since the outer peak does not emerge in the streamwise spectra at the present Reynolds number. Thus, the spanwise wavelength λ_z/R=0.5 is settled as the cutoff criterion for the effective scale-separation between the large- and small-scale motions.

Two-point AM covariance was calculated to investigate the effects of the large-scale structures on the small-scale structures, and is shown in figure 7. A clear symmetric contour is present with respect to the diagonal line at Re_τ=180, but anti-symmetric contours appear at higher Reynolds numbers. The symmetries disintegrate due to the emergence of the secondary peak in the logarithmic region at $y_1^+\approx100$ and the viscous and buffer layers at $y_2^+\approx10$. This peak results from the non-linear AM signature, for which the large-scale structures in the logarithmic region impose obvious imprints on the near-wall region (Mathis et al., 2009a). The interesting feature is that the peak strength increases with increasing the Reynolds number. Therefore, this conclusion implies that the active AM mechanism results in increases in the inner-scaled near-wall peak in turbulent flows. This conflicts with the previous results for pipe flows that the energy contribution in pipe flows of the large-scale structures to the near-wall small-scale structures is different from that in TBLs (Monty et al. 2009; Hultmark et al., 2010; Hultmark et al., 2012).

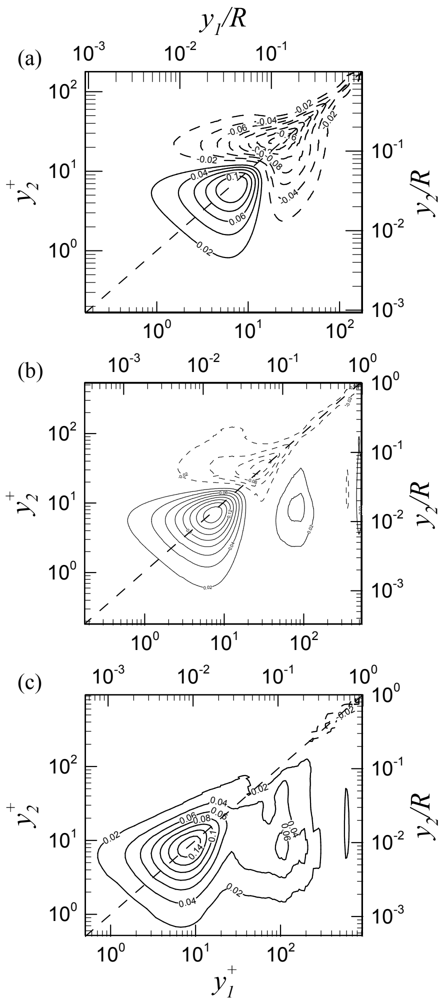

Figure 7: Two-point AM covariances for (a) Re_τ=180, (b) Re_τ=544 and (c) Re_τ=934.

CONCLUSIONS

We carried out the DNSs of fully developed turbulent pipe flows to investigate the inner-scaled turbulence statistics and the interactions between the near-wall and outer regions for the Reynolds numbers Re_τ=180, 544, and 934. The mean streamwise velocity with respect to the Reynolds number showed not only the existence of the logarithmic region except for the lowest Reynolds number but also the increasing wake strength with the Reynolds numbers. The near-wall peaks in the turbulence intensities were shown to increase with the Reynolds number. In particular, the streamwise near-wall peak intensity was found to be quantitatively similar to those found in TBL and channel flows, even in the magnitude and growth rate. To corroborate the present findings, spectral analyses were conducted. The pre-multiplied streamwise energy spectra at y^+≈15 showed that the long-wavelength energy magnitude grows with the Reynolds number, although the small-scale energy well collapsed, providing the evidence for the increasing inner-scaled peak intensity. It was also found by the inspection of the AM signatures that as the Reynolds number increases, a secondary peak appears and becomes stronger due to the non-linear AM effect. The increase of the near-wall streamwise peak intensity was therefore originated from the increase of the large-scale energy in the near-wall region that arises from the penetration of the large-scale structures present in the logarithmic region. Since the trends of the inner-scaled near-wall peak in the streamwise intensity were similar irrespective of the flow type, such as external or internal flows, even with magnitude and increasing rate, we finally concluded that there might be an identical interaction between the inner and outer flows in the canonical wall-bounded turbulent flows.

ACKNOWLEDGEMENT

This work was supported by the Creative Research Initiatives program (No.2013-0003364) of the National Research Foundation of Korea and was partially supported by KISTI under the Strategic Supercomputing Support Program.

REFERENCES

Akselvoll, K. & Moin, P., 1996, “Large-eddy simulation of turbulent confined coannular jets,” *J. Fluid Mech.* 315, 387-411.

Bernardini, M. & Pirozzoli, S., 2011, “Inner/outer layer interactions in turbulent boundary layers: A refined measure for the large-scale amplitude modulation mechanism,” *Phys. Fluids* 23, 061701.

Chin, C., Ooi, A.S.H., Marusic, I. & Blackburn, H.M., 2010, “The influence of pipe length on turbulence statistics computed from direct numerical simulation data,” *Phys. Fluids* 22, 115107.

Hoyas, S. & Jiménez, J., 2006, “Scaling of the velocity fluctuations in turbulent channel up to Re_τ=2003,” *Phys. Fluids* 18, 011702.

Hultmark, M., Bailey, S.C.C. & Smits, A.J., 2010, “Scaling of near-wall turbulence in pipe flow,” *J. Fluid Mech.* 649, 103-113.

Hultmark, M., Vallikivi, M., Bailey, S.C.C. & Smits, A.J., 2012, “Turbulent pipe flow at extreme Reynolds numbers,” *Phys. Rev. Lett.* 108, 094501.

Hutchins, N. & Marusic, I., 2007a, “Evidence of very long meandering features in the logarithmic region of turbulent boundary layers,” *J. Fluid Mech.* 579, 1-28.

Hutchins, N. & Marusic, I., 2007b, “Large-scale influences in near-wall turbulence,” *Phil. Trans. R. Soc. A* 365, 647-664.

Hutchins, N., Nickels, T.B., Marusic, I. & Chong, M.S., 2009, “Hot-wire spatial resolution issues in wall-bounded turbulence,” *J. Fluid Mech.* 635, 103-136.

Jang, S.J., Sung, H.J. & Krogstad, P.-A., 2011, “Effects of axisymmetric contraction on a turbulent pipe flow,” *J. Fluid Mech.* 687, 376-403.

Kim, J., Moin, P. & Moser, R., 1987, “Turbulence statistics in fully developed channel flow at low Reynolds number,” *J. Fluid Mech.* 177, 133-166.

Kim, K.C. & Adrian, R.J., 1999, “Very large-scale motion in the outer layer,” *Phys. Fluids* 11, 417–422.

Kim, K., Baek, S.–J. & Sung, S.J., 2002, “An implicit velocity decoupling procedure for the incompressible

Navier-Stokes equations," *Int. J. Numer. Method Fluids* 38, 125–138.

Ligrani, P.M. & Bradshaw, P., 1987, "Spatial resolution and measurement of turbulence in the viscous sublayer using subminiature hot-wire probes," *Exp. Fluids* 5, 407-417.

Marusic, I. & Kunkel, G.J., 2003, "Streamwise turbulence intensity formulation for flat-plate boundary layers," *Phys. Fluids* 15, 2461–2464.

Mathis, R., Hutchins, N. & Marusic, I., 2009a, "Large-scale amplitude modulation of the small-scale structures in turbulent boundary layers," *J. Fluid Mech.* 628, 311-337.

Mathis, R., Monty, J.P., Hutchins, N. & Marusic, I., 2009b, "Comparison of large-scale amplitude modulation in turbulent boundary layers, pipes, and channel flows," *Phys. Fluids* 21, 111703.

Monty, J.P., Hutchins, N., Ng, H.C.H., Marusic, I. & Chong, M.S., 2009, "A comparison of turbulent pipe, channel and boundary layer flows," *J. Fluid Mech.* 632, 431-442.

Moser, R.D., Kim, J. & Mansour, N.N., 1999, "Direct numerical simulation of turbulent channel flow up to Re_τ=590," *Phys. Fluids* 11, 943-945.

Ng, H.C.H., Monty, J.P., Hutchins, N., Chong, M.S. & Marusic, I., 2011, "Comparison of turbulent channel and pipe flows with varying Reynolds number," *Exp. Fluids* 51, 1261-1281.

Schlatter, P. & Örlü, R., 2010a, "Quantifying the interaction between large and small scales in wall-bounded turbulent flows: A note of caution," *Phys. Fluids* 22, 051704.

Schlatter, P. & Örlü, R., 2010b, "Assessment of direct numerical simulation data of turbulent boundary layers," *J. Fluid Mech.* 659, 116–126.

Wu, X. & Moin, P., 2008, "A direct numerical simulation study on the mean velocity characteristics in turbulent pipe flow," *J. Fluid Mech.* 608, 81-112.

Wu, X., Baltzer, J.R. & Adrian, R.J., 2012, "Direct numerical simulation of a 30*R* long turbulent pipe flow at R^+= 685: large- and very large-scale motions," *J. Fluid Mech.* 698, 235-281.